Acta Pharmacol Sin 2009 Jun; 30 (6): 859–867

Original Article

Nonlinear dynamical analysis of carbachol induced hippocampal oscillations in mice

Metin AKAY[1,*], Kui WANG[2], Yasemin M AKAY[1], Andrei DRAGOMIR[1], Jie WU[2]

[1]Harrington Department of Bioengineering, Ira A. Fulton School of Engineering, Arizona State University, Tempe, AZ 85287, USA; [2]Division of Neurology, Barrow Neurological Institute, Phoenix, AZ 85013, USA

Aim: Hippocampal neuronal network and synaptic impairment underlie learning and memory deficit in Alzheimer's disease (AD) patients and animal models. In this paper, we analyzed the dynamics and complexity of hippocampal neuronal network synchronization induced by acute exposure to carbachol, a nicotinic and muscarinic receptor co-agonist, using the nonlinear dynamical model based on the Lempel-Ziv estimator. We compared the dynamics of hippocampal oscillations between wild-type (WT) and triple-transgenic (3xTg) mice, as an AD animal model. We also compared these dynamic alterations between different age groups (5 and 10 months). We hypothesize that there is an impairment of complexity of CCh-induced hippocampal oscillations in 3xTg AD mice compared to WT mice, and that this impairment is age-dependent.
Methods: To test this hypothesis, we used electrophysiological recordings (field potential) in hippocampal slices.
Results: Acute exposure to 100 μmol/L CCh induced field potential oscillations in hippocampal CA1 region, which exhibited three distinct patterns: (1) continuous neural firing, (2) repeated burst neural firing and (3) the mixed (continuous and burst) pattern in both WT and 3xTg AD mice. Based on Lempel-Ziv estimator, pattern (2) was significantly lower than patterns (1) and (3) in 3xTg AD mice compared to WT mice (P<0.001), and also in 10-month old WT mice compared to those in 5-month old WT mice (P<0.01).
Conclusion: These results suggest that the burst pattern (theta oscillation) of hippocampal network is selectively impaired in 3xTg AD mouse model, which may reflect a learning and memory deficit in the AD patients.

Keywords: hippocampus; oscillations; carbachol; Lempel-Ziv complexity; 3xTg AD mice; electrophysiology
Acta Pharmacologica Sinica(2009) 30: 859–867; doi: 10.1038/aps.2009. 66

Introduction

Carbachol is poorly absorbed through the gastrointestinal tract and never crosses the blood-brain barrier. Carbachol is a parasympathomimetic compound that stimulates both nicotinic and muscarinic receptors[1, 2]. Carbachol, a cholinergic agonist, induces rhythmic oscillations in pyramidal neurons in the CA1 and CA3 hippocampal areas through the activation of class I interneurons using multiple collaterals. GABA-A (γ amino butyric acid-A) receptors are essential in keeping the carbachol oscillations' repeatability[3]. Another study claimed that glutamatergic neurons' afferent fibers are responsible for the class I interneurons' rhythmic excitation[4].

One study used carbachol as a muscarinic receptor agonist to activate three different oscillation types in the CA3 region in rat hippocampal slices. It stimulated synchronous discharges (called carbachol-delta) using low concentrations (4–13 μmol/L), while higher concentrations (13–60 μmol/L) activated a very distinctive oscillation patterns (called carbachol-theta)[5]. Researchers have shown that, carbachol, when applied between 8–25 μmol/L, can also activate spontaneous γ oscillation episodes again in the CA3 area of hippocampal slices[5–7], which is mediated by the activation of GABA-A and AMPA (α-amino-3-hydroxy-5-methyl-4-isoxazolepropionic acid) receptors[8]. Furthermore, carbachol is proven to induce β-oscillations in the hippocampal slices[9]. A recent study that characterizes carbachol oscillation's pharmacological and cellular features in the rat hippocampal slice suggested that the oscillations in CA1 area need the CA3 region's synaptic propagation for initiating the carbachol oscillations[10, 11].

Carbachol also induces 40 Hz oscillations in the slices

* Correspondence to Dr Metin AKAY, PhD.
E-mail Metin.Akay@asu.edu
Received 2009-03-03 Accepted 2009-04-20

taken from hippocampal CA3 region. The oscillatory electrical activity can be observed as a response to many different stimuli in the CA3 region's pyramidal cells of the hippocampal slice. Carbachol oscillations have similar frequencies with these oscillations, called "θ-rhythm" *in vivo*. A successful *in vitro* model of those oscillations should show similar cell-cell interactions as *in vivo* structures[11, 12].

Traub *et al* has suggested that, in many epilepsy models, the features of carbachol oscillations are akin to the epileptiform bursts than to the θ-rhythm[13]. Scanziani *et al* stated that carbachol oscillations in the CA3 region's neurons in the hippocampus exhibited a more controlled behavior than other sites of epileptiform bursting. This could be because the glutamate release by the muscarinic receptors on the CA3 nerves is partially suppressed[14].

Nicotinic acetylcholine receptors (nAChRs) are a group of ligand-gated ion channels that play an important role in many of the brain's cognitive functions[15]. Alzheimer's disease (AD) is a neurological disorder that progressively destroys cognitive function. At the cell level, cholinergic neurotransmission deficits such as decrease in ACh (acetylcholine) release and choline acetyltransferase activity, and cholinergic neuron loss in the basal forebrain occur early in AD, leading to cognitive impairment[16]. Other distinctive characteristics of AD are intracellular neurofibrillary tangles made of tau protein and extracellular neuritic plaques made of the β-amyloid peptide (A-Beta1-42)[16]. Pettit *et al* investigated A-Beta1-42's role on nAChR currents in the rat hippocampal slice, since this is the brain's primary area for cognitive tasks. Nicotinic currents stimulated by the local photolysis of caged-carbachol are blocked by A-Beta1-42 binding to nAChRs[17]. These researchers further explored that this inhibition is applied by the peptide fragment that includes amino acid residues 12-28, by the A-Beta12-28 part of the A-Beta1-42[18].

Liu and Wu further suggested that soluble A-Beta is more associated with cognitive decline in AD patients than insoluble fibril deposits, which has been also confirmed by the studies in APP transgenic mouse models[19]. Goto *et al* showed that carbachol reduced the field excitatory postsynaptic potentials (fEPSPs) in the hippocampal CA1 region in both wild-type and transgenic mice at 5 μmol/L concentration[20]. Auerbach and Segal reported similar results, suggesting that reduced field EPSPs were because of presynaptic muscarinic acetylcholine receptor stimulation in rat hippocampus with the effect of carbachol in micromolar concentrations[21].

Physiological signals have a wide variety of forms. To describe them, traditional feature measures typically extract amplitude and frequency information. This makes comparison of signals which have different bandwidths difficult[22]. In addition, such measures do not allow comparison within subject groups, as the absolute frequency of rhythms may differ from person to person, and may depend on other factors such as patient sex and age. Hence, additional analysis methods are needed to be developed. When visually inspecting signals, one of the first impressions is their "complexity." In the present study, we have analyzed the complexity and the dynamics of carbachol-induced neuronal oscillations in the hippocampal CA1 area in both WT and 3xTg AD mice with 5- and 10-month old ages by utilizing the Lempel-Ziv (LZ) method.

Materials and methods

Hippocampal slice preparation Hippocampal slices were prepared from 5- and 10 month-old mice that were sacrificed in accordance with Institutional Animal Welfare Committee guidelines, as previously described[23, 24]. After isoflurane-induced anesthesia, brain tissue was quickly removed and bathed in cold (4 °C) artificial cerebrospinal fluid (ACSF) containing (in mmol/L): 135 NaCl, 3 KCl, 16 $NaHCO_3$, 1 $MgCl_2$, 1.25 NaH_2PO_4, 2 $CaCl_2$, and 10 glucose, bubbled with 95% O_2–5% CO_2 (carbogen). This specific ACSF composition was chosen because it has been successfully used in previous γ oscillation studies[25–28]. Using a vibratome (Vibroslice 725 M, WPI, Sarasota, FL, USA), several 400-μm transverse coronal sections containing the dorsal hippocampus were cut, transferred to a holding chamber and were incubated at room temperature (22±1 °C) for at least 60 min in ACSF prior to recording. Next, one slice was transferred to a liquid-air interface chamber (Fine Science Tools Inc, Foster City, CA, USA) and was suspended on a nylon net at the liquid-air interface in a bath of continuously dripping ACSF (2–2.5 mL/min) bubbled with carbogen. Humidified carbogen was passed along the upper surface of the slice and bath temperature was regulated by a feedback circuit accurate to 0.5±0.2 °C. Baseline temperature was 34±1 °C. Carbachol (CCh) was the chemical used in this study and was purchased from Sigma.

Electrophysiological recordings Standard extracellular field potential recordings were performed from the hippocampal CA1 cell layer using borosilicate glass micropipettes pulled to a 1 mm tip diameter and filled with 2 mol/L NaCl[23, 24]. Recordings were made using an Axoclamp-2B amplifier (Axon Instruments Inc, Union City, CA, USA). CCh was applied continuously during recording period. The CCh was dissolved in ACSF, and the drug solution was

dripped at the same rate into the bath as drug-free ACSF (2–2.5 mL/min). Washout was accomplished by switching from the dripping solution containing the drug to the drug-free ACSF. The drug application's effects were observed 20–60 min after perfusion.

Data acquisition and analysis Data were acquired by pClamp 9 via an Axon Digidata 1322 (Axon Instruments, Inc, Union City, CA, USA) interface board set to a 10 kHz sampling frequency, filtered in Clampex 9.0 using an 8-pole Bessel filter and a 1-kHz low-pass filter, and stored on hard media for subsequent off-line analysis. The induced response's power in the frequency spectrum was calculated off-line using Fast Fourier Transform (FFT) in Clampfit software 9.0 (Axon Instruments). Statistical comparisons of results were performed using Origin 5.0 (Microcal Software, Inc, Northampton, MA). Spike counting was performed off-line using Clampfit by setting a threshold of 3 times baseline noise. Prior to having the program count the number of spikes, those above threshold were manually confirmed. Waveforms having an interspike interval (ISI) under 12.5 ms (frequency greater than 80 Hz) were excluded. Also, no further spikes were considered after two or more consecutive ISIs over 33.3 ms had been identified.

Lempel-Ziv complexity Synaptic connections between CA1 and CA3 neurons trigger the neural oscillations induced by carbachol, resulting in rhythmic excitation of CA1 region. Thus, the rhythmic activity we recorded from hippocampal neurons arise from complex feedback networks and non-linear interconnections that are characteristic for such physiological systems. We used the Lempel-Ziv (LZ) complexity estimator to analyze our recordings. Traditional analysis techniques (*eg* Fourier, power spectra) can't capture neural oscillations dynamics. Thus we used the LZ complexity, which quantifies the new pattern generation rate along given sequences of symbols, as a measure of the oscillation complexity (regularity)[29–32]. LZ complexity is similar to information theoretic methods such as entropy[31] and can cope with discrete-time symbolic sequences. The use of symbolic representations of time series data is particularly favored when low amplitude noise hampered the data. Thus, we transformed the neural signals into finite sequences in the symbolic space, which was perfectly suitable because of the particularities of our recordings. Each sample in the time domain was assigned a symbol and the total number of unique symbols forms the sequence's alphabet. Since the data was composed of long series of field events (spikes) in the extracellular recordings, that form the oscillation response of the neurons when presented with the cholinergic agonist carbachol, we used a binary alphabet. The time axis was divided into discrete bins. The field events were detected using an amplitude threshold and each time the threshold was crossed, we placed a "1" in the respective bin of the symbolic representation of our signals. For all bins with values below the threshold were assigned as "0"[32].

Our signal x(n) was formally converted into a binary sequence $S=s(1), s(2), \ldots, s(n)$ where:

$$s(i)=\begin{cases} 0, \textit{if } x(i)<T \\ 1, \textit{otherwise} \end{cases}$$

where T is the threshold, in our case $2\cdot\sigma(x(n))$, where σ denotes the standard deviation of the signal[32].

When computing the LZ complexity, the sequence S is parsed from left to right and a complexity counter $c(n)$ is increased whenever a new subsequence (distinct word) is encountered. The algorithm followed is: (a) Let $S(i,j)$ denote a substring of S that starts at position i and ends at position j, where $i<j$, $S(i,j)=s_i s_{i+1}\cdots s_j$ and when $i > j$, $S(i,j)=\{\}$. The vocabulary of the sequence S, $V(S)$, is the set of all unique substrings (words) $S(i,j)$ of S. (b) The parsing procedure starts by comparing a substring $S(i,j)$ to the vocabulary that is comprised of all substrings of S up to $j-1$, that is $V(S(1,j-1))$. If $S(i,j)$ is present in $V(S(1,j-1))$ then update $S(i,j)$ and $V(S(1,j-1))$ to $S(i,j+1)$ $V(S(1,j))$, respectively and repeat the previous check. If the substring is absent, place a dot after $S(j)$ to indicate the end of a new component, update $S(i,j)$ and $V(S(1,j-1))$ to $S(j+1,j+1)$ and $V(S(1,j))$, respectively and the process continues. The whole parsing operation begins at $S(1,1)$ and continues until $j=n$, the total length of the binary sequence[30].

For example, the sequence S=1011110100010 is parsed as 1·0·11·110·100·010. Therefore, the vocabulary of S is 6. Similarly, a sequence S=0001101001000101 would be parsed as 0·001·10·100·1000·101, and hence yield a vocabulary sized 6 (see[29] for details).

The LZ complexity is defined as the total number of words in the decomposition, $c(n)$. The normalized LZ complexity is defined as:

$$C_{LZ}=\frac{c(n)}{n/\log_2 n}$$

More details on the LZ method and its implementation are given elsewhere[29].

Results

The bath application of carbachol (100 μmol/L) generated extracellularly recorded field events (oscillations), which were recorded for at least 60 min. The oscillations presented three distinct pattern types, one consisting of individual field

events that were grouped into regularly spaced bursts with high firing rate (>3 Hz), second, with long-lasting periods of continuous low firing rate activity with relatively constant frequency (<1 Hz), and third one is a mixture of the continuous firing with burst. The bursting-type patterns are typically referred to as carbachol oscillations and can be recorded in either *S pyramidale* or *S radiatum*[33]. The carbachol oscillations may represent population spikes fired synchronously from multiple pyramidal cells[23, 24, 33].

We recorded data from 72 hippocampal slices taken from eight wild-type (WT) and six 3xTg AD mice aged 5 and 10 months (n=5 for the 5-month aged WT group, n=3 for the 10-month aged WT group, n=3 for both the 5- and 10- month aged 3xTg groups). We generally observed more burst-type activity in the young age group (5 months) and in the wild-type (WT) mice, when compared to old (10 months) and 3xTg AD mouse counterparts. Figure 1 shows typical traces of the two neural activity patterns that were recorded from a 5 months old WT (A and B) or 3xTg AD (C and D) mouse, respectively. Figure 2 presents the corresponding raw traces from WT (A and B) and 3xTg AD (C and D) mouse at 10 months age. Bursting duration ranged generally from 5 to 10 s. The system transitioned between the two states (of continuous and burst-type activity), with neural activity of highly irregular firing rate lasting 2–3 min. This transition might be a stage during which the neural activity undergoes reorganization, reflected by the corresponding random patterns of oscillation. Figure 3 presents

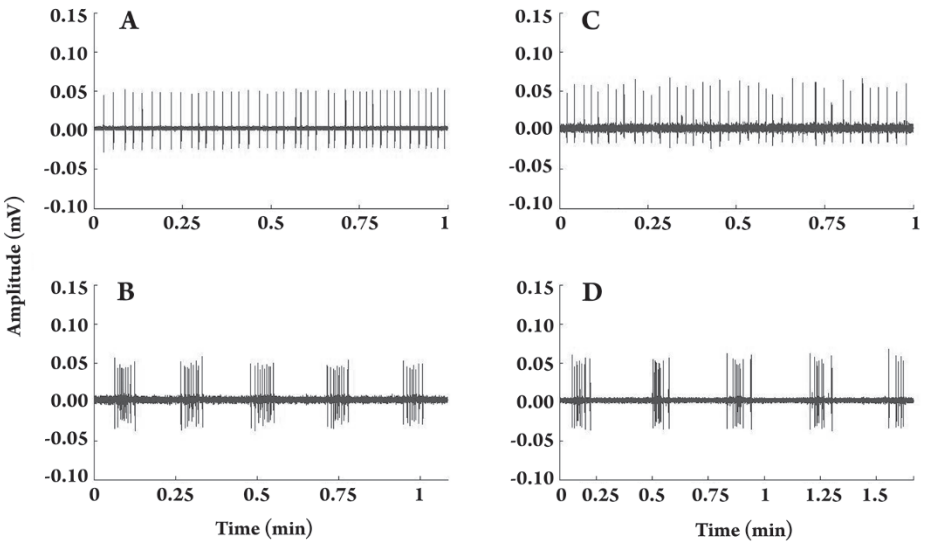

Figure 1. Typical recordings from two 5 months old mice: Wild-Type (A and B) and Transgenic (C and D). A and C: Continuous type activity of very low firing rate. B and D: regularly spaced burst formations of higher firing rate (>3 Hz).

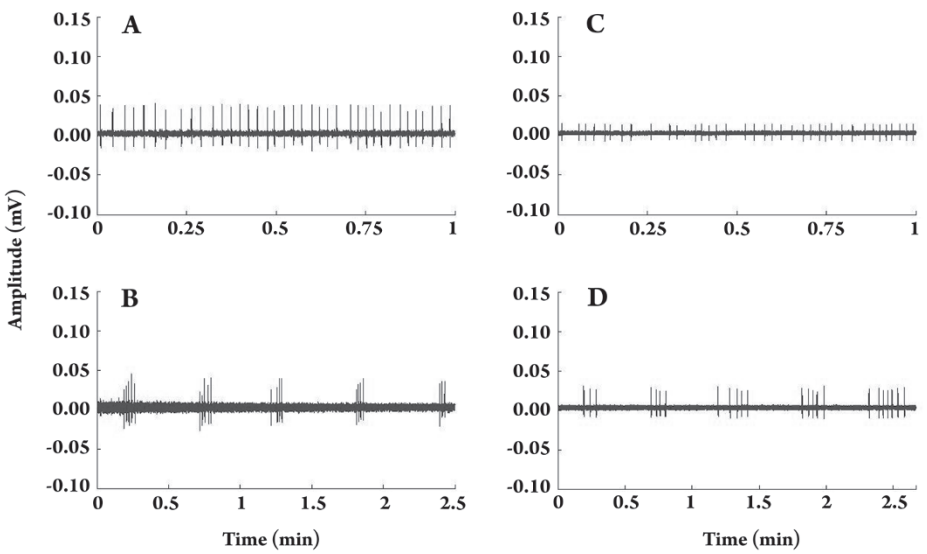

Figure 2. Typical recordings from two 10 months old mice: Wild-Type (A and B) and Transgenic (C and D). A and C: Continuous type activity of very low firing rate. B and D: regularly spaced burst formations of higher firing rate (>3 Hz).

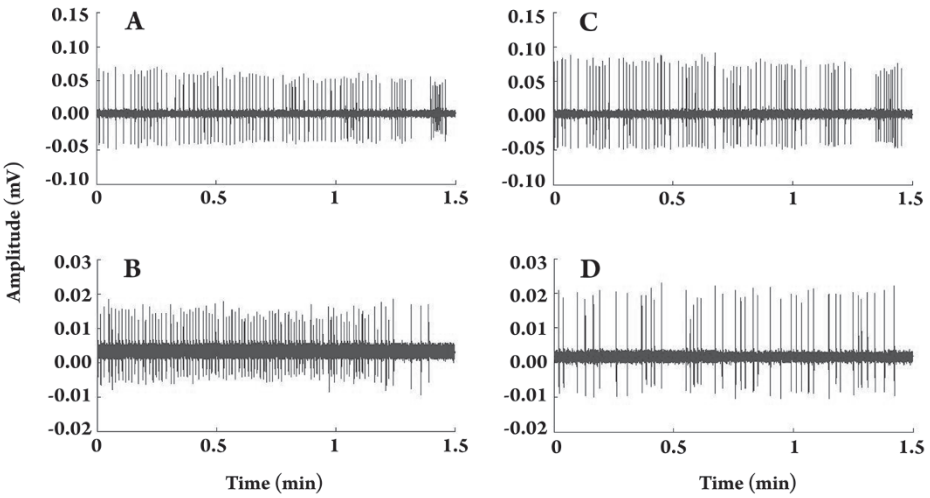

Figure 3. Typical recordings during transition from continuous to burst type neural activity: Wild-Type (A and B) and Transgenic (C and D). A and C: 5-month-old mouse. B and D: 10-month-old mouse.

typical transitional neural activity traces from a 5 month-old (panels A and C) and a 10 month-old mouse (panels B and D), respectively. The left side panels correspond to WT and the right side panels to the 3xTg AD mouse. We observed no neural activity during the control experiments (no drug applied).

We further analyzed the carbachol's effects on the complexity of the hippocampal oscillations in WT and 3xTg AD mice using the LZ estimator. For this analysis, the segments of 1 min were taken during the continuous-type activity from records exhibiting more than 3 min of relatively constant firing rate (as shown in Figure 1 and 2, panels A and C). We also selected 5 consecutive bursts from each recording exhibiting bursting type activity.

The procedure was repeated for both age groups in WT and 3xTg AD mice. As shown in Figure 4, the complexity values of continuous-type neural activity segments were similar when comparing WT and 3xTg AD mice. The old age group's values were slightly (but immaterially) smaller than the young group. However, when examining the burst-type activity's complexity (Figure 5), the patterns changed dramatically. The difference in the WT case is lower but still significant (P<0.01). The complexity values for the 3xTg AD mice were decreased with a drastic drop in the case of the 10-month-old age group (significant, with P<0.001).

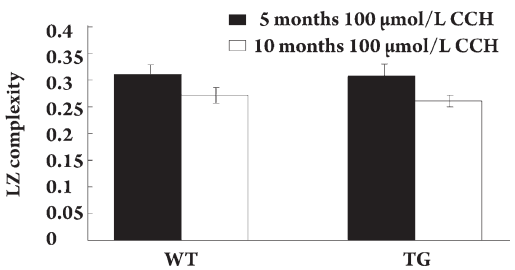

Figure 4. Complexity values for continuous type neural activity. Values correspond to complexity averages (±SEM) of 1 min long recording segments taken from each of the 14 mice ($n_{WT\_10\ months}$=$n_{WT\_5months}$=34, $n_{TG\_10\ months}$=$n_{TG\_5\ months}$=28).

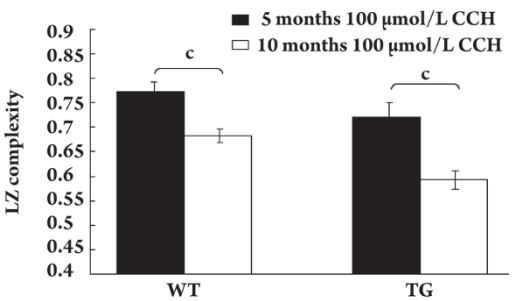

Figure 5. Complexity values for burst-type neural activity. Values correspond to complexity averages (±SEM) of 5 consecutive bursts taken for each of the 14 mice ($n_{WT\_10\ months}$=$n_{WT\_5\ months}$=45 and $n_{TG\_10\ months}$=$n_{TG\_5\ months}$= 20). $^c P$<0.01.

Figure 6 shows the complexity values of 1 min long signal segments during transition phase. The differences between the complexities of young and old age group are irrelevant for both WT and 3xTg AD mice.

Discussion

In the present study, we proposed a novel nonlinear dynamical analysis method based on the LZ complexity method to analyze hippocampal oscillations induced by acute carbachol exposure on hippocampal slices in WT and

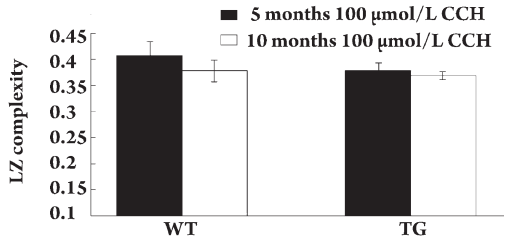

Figure 6. Complexity values for transitional neural activity. Values correspond to complexity averages (±SEM) of 1 min long recording segments taken from each of the 14 mice ($n_{WT\_10\ months}$=$n_{WT\_5\ months}$=12 and $n_{TG\_10\ months}$=$n_{TG\_5\ months}$=18).

3xTg AD mice. By using this mathematic analysis, we are able to quantitatively distinguish three patterns from hippocampal neuronal oscillations. These patterns may reflect different status of neuronal network synchronization. More importantly, the analysis using the non-linear mathematic model (LZ complexity estimator) demonstrates that only burst pattern exhibits significant impairment in 3xTg AD mice and this impairment is likely age-dependent.

The neural oscillations recorded from hippocampus neurons arise from complex feedback networks and non-linear interconnections, which are characteristic for physiological systems. Traditional analysis techniques (*eg* Fourier, power spectra) may not capture the dynamics of neural oscillations[22, 34]. A series of methods have been used to investigate the properties of biomedical signals, such as the Shannon entropy (ShEn), spectral entropy (SpEn), approximate entropy (ApEn), Lempel-Ziv complexity (LZ), or Higuchi fractal dimension (HFD). Ferenets *et al*[34] provided an extensive comparison of different entropy and complexity measures using surrogate signals as well as real EEG signals[34]. Their study is especially interested in the sensitivity of the mentioned measures to the bandwidth of the signal spectrum and the shape of the probability density function (PDF). They showed that ShEn does not depend on signal bandwidth as could be expected from the definition of this measure. The SpEn, in contrary to ShEn, does not depend on the shape of the signal's PDF. ApEn depends on both the shape of the PDF as well as the spectral bandwidth of the signal. At sharp PDFs, ApEn behaves similarly to ShEn with respect to the shape of the PDF (given that the bandwidth is large enough). As the signal amplitude becomes more uniformly distributed, ApEn values stay constant, depending only on the spectral bandwidth. Also, the ApEn values slightly increase with increasing signal length. The behavior of LZ complexity and HFD look similar. Both parameters depend mainly on the bandwidth of the signal spectrum (less than the other measures, however) while slight dependence on the PDF can be observed mostly when the parameters controlling PDF's sharpness is small.

Additionally, Ferenets *et al*[34] showed that while LZ complexity, ApEn, and HFD are relatively independent of the amount of data (window length), SpEn and, in some cases, ShEn, show significant trend. This comes from the fact that ShEn and SpEn both use transformation over the Shannon function. The same study concludes that methods based on the phase space background (ApEn and HFD) or pattern recurrence (LZ complexity) seems to have slight advantage in analyzing the EEG signals. Their results clearly show that the various parameters called entropy actually measure different properties of the signal. ShEn, the "classical" entropy measure, does not depend on signal spectrum while SpEn is insensitive to the amplitude distribution (which is easy to predict from the mathematical formulas defining these parameters). However, LZ complexity seems to be more suitable when dealing with finite symbol and discrete time signals, as it can be expected from its mathematical formula.

As noted by several authors, the complex feedback networks and nonlinear couplings inherent in the physiological system give rise to characteristic oscillations[35–37]. Nagarajan *et al*[37] pointed out that while the system is undisputedly nonlinear, it is far from trivial whether this nonlinearity is exhibited in the external recording. The oscillations in these recordings can be either due to a nondeterministic component or a nonlinear deterministic component. Traditional techniques such as Fourier analysis fail to provide adequate information regarding the dynamics of the data. For instance, it is possible to generate two data sets, which have similar spectra but different dynamics. The search for alternate measures to quantify the dynamics has been an area of recent interest.

The use of symbolic techniques to map a time series into a sequence retaining its dynamics has been quite popular[38–57]. The robustness of the resulting symbolic representation to low amplitude noise is also appreciated[40–42]. The fundamental idea is to partition the samples in the real space into a finite sequence in the symbol space. Each sample in the original data is assigned a unique symbol and the number of distinct symbols forms the alphabet set of the sequence. The regularity of the resulting sequence is quantified using a chosen complexity measure.

The LZ complexity has been applied extensively in biomedical signal analysis as a metric to estimate the complexity of discrete-time physiologic signals, proving its robustness when over other complexity/entropy measures. For instance, LZ has been used for recognition of structural

regularities[42], for complexity characterization of DNA sequences[45–47], to develop new methods for discovering patterns in DNA sequences by applying it to genomic sequences of Plasmodium falciparum[47], and to estimate the entropy of neural discharges (spike trains)[48, 49]. LZ complexity has also been used to study brain function[51], brain information transmission[52], and EEG complexity in patients with Alzheimer's disease[53], and epileptic seizures[54]. Other authors have used LZ complexity to study ECG dynamics[55], Generally, previous work involving the application of LZ in the context of biomedical signal analysis has consisted of analyzing signals from a specific patient population or pathology, and identifying a LZ change associated with a specific condition of interest[56]. The fact that LZ quantifies primarily the signal bandwidth and bandwidth of the signal harmonics is relevant in biomedical signal analysis[29].

Due to its robustness, LZ complexity has also found applications to the neural recordings. Szczepanski *et al*[57] present three applications of LZ complexity to the analysis of spike trains: (i) estimation of the entropy, (ii) discrimination of neural responses via complexity curves and (iii) discrimination of neural responses via the number of states of the corresponding neuronal sources. Additionally, Amigo *et al*[49] used LZ for estimating the entropy rate of spike trains and underlined that LZ is closely related to such important source properties as entropy and compression ratio, but in contrast to these, it is a property of individual sequences [49].

Previous studies[58–62] in transgenic (Tg) mice models of Alzheimer's Disease (AD) point out the presence of quite a number of beta-amyloid deposit in the hippocampus and other brain areas as well as cholinergic dysfunction and impairment in learning and memory functions. Therefore a vast amount of research has been done to make a comparison between the 7 month-old Tg and WT (wild type) mice in terms of the intracellular pathways that might be switched on/off in the hippocampal areas. One of the major pathways that have been proven to be responsive to inflammatory stimuli, environmental stress or other insults is ERK (extracellular regulated kinase)[63]. It has been widely accepted that activation of ERK is very closely related to memory formation[64–67]. Since it has been shown in many systems that, ERK activation is downstream of cholinergic stimulation through both nicotinic[65] and muscarinic[66] receptors, a research has been done to determine whether cholinergic stimulation might activate ERK differently in the hippocampus of Tg and WT mice. Cholinergic stimulation with CCh (carbachol) has shown a strong increase in ERK activation in the CA1 (cornu ammonis area 1) pyramidal neurons of WT mice while this effect is significantly less dense in the hippocampus of Tg mice, pointing out a possible mechanism responsible for the presence of memory deficits [58] in them because of the strong connections between the ERK pathway and the cholinergic system in memory functions [68].

All these previous studies encouraged us to use this novel nonlinear dynamical analysis method, based on the LZ complexity method, to analyze hippocampal oscillations induced by acute carbachol exposure on hippocampal slices in WT and 3xTg AD mice. Our analysis demonstrated that the complexity values of continuous patterns in response to carbachol were almost the same for the 5-month old wild and transgenic mice. But, they were decreased in the 10-month old wild and transgenic mice, but these differences were not statistically significant. On the other hand, the complexity values of burst patterns were smaller for the 5-month old transgenic mice compared to those of 5-month wild mice and were significantly smaller in the 10-month wild and transgenic mice. Thus, the difference was much more drastic for the transgenic mice. Finally, the complexity values of the mixed patterns were more or less the same for the 5- and 10-month old wild and transgenic mice. The difference in the WT case is lower but still significant (P<0.01). We speculate that the reason for the drastic drop in the complexity of burst-type neural activity of TG mice is the declined cholinergic neurotransmission that has been reported in TG mouse models in several studies. This neurotransmission deterioration was shown to be caused by the formation of amyloid β–peptide deposits[59–61]. The even larger decrease in complexity values that we observed in our data for the older group matches with results that indicate the deterioration to be age-dependent[59, 60].

Therefore, our analysis indicates that the LZ based complexity estimator is a useful tool for the characterization of the dynamical changes in hippocampal oscillations. It is well known that neuronal synchronization deficits, especially theta oscillation, are correlated to learning and memory deficit in the AD patients. As demonstrated in our mathematical analysis, such attenuation could be quantitatively represented as an impairment of burst pattern firing during exposure to CCh. Therefore, our analysis not only provides a convinced way to evaluate the nature of hippocampal neuronal oscillations, but also may open a new window to help the diagnosis of AD, to evaluate pathological status of AD and also to evaluate the effects of the medical therapy of the AD.

Author contribution

Jie WU and Kui WANG designed research; ALL the authors performed research; Metin AKAY,Andrei DRAG-

MIR and Yasemin M AKAY contributed new analytical tools and reagents; Metin AKAY, Andrei DRAGOMIR and Yasemin M AKAY analyzed data; Metin AKAY, Yasemin M AKAY, Andrei DRAGOMIR,and Jie WU wrote the paper.

References

1 Brenner GM. Pharmacology, Philadelphia (PA): W.B. Saunders Company; 2000.
2 Canadian Pharmacists Association. Compendium of pharmaceuticals and specialties (25th ed). Toronto (ON): Webcom; 2000.
3 Williams JH, Kauer JA. Properties of carbachol-induced oscillatory activity in rat hippocampus. J Neurophysiol 1997; 78: 2631–40.
4 Dickson CT, Alonso A. Muscarinic induction of synchronous populationactivity in the entorhinal cortex. J Neurosci 1997; 17: 6729–44.
5 Fellous1 JM, Sejnowski TJ. Cholinergic induction of oscillations in the hippocampal slice in the slow (0.5–2 Hz), theta (5–12 Hz), and gamma (35–70 Hz) bands. Hippocampus 2000; 10: 187–97.
6 Fellous JM, Johnston T, Segal M, Lisman JE. Carbachol-induced rhythms in the hippocampal slice: slow (5–2 Hz), theta (4–10 Hz) and gamma (80–100 Hz) oscillations. In: Bower JM, Editor. Computational neuroscience: trends in research. New York: Plenum Press; 1998. p367–372.
7 Natsume K, Kometani K. Theta activity-dependent and –independent muscarinic facilitation of long-term potentiation in guinea pig hippocampal slices. Neurosci Res 1997; 27: 335–41.
8 Fisahn A, Pike FG, Buhl EH, Paulsen O. Cholinergic induction of network oscillations at 40 Hz in the hippocampus *in vitro*. Nature 1998; 394: 186–9.
9 Shimono K, Brucher F, Granger R, Lynch G, Taketani M. Origins and distribution of cholinergically induced beta rhythms in hippocampal slices. J Neurosci 2000; 20: 8462–73.
10 Zhang L, Liu Y, Chen X. Carbachol induces burst firing of dopamine cells in the ventral tegmental area by promoting calcium entry through l-type channels in the rat. J Physiol 2005; 568: 469–81.
11 Traub RD, Miles R, Buzsaki G. Computer simulation of carbachol-driven rhythmic population oscillations in the ca3 region of the *in vitro* rat hippocampus. J Physiol (Lond) 1992; 451: 653–72.
12 Traub RD, Borck C, Colling SB, Jefferys JGR. On the structure of ictal events *in vitro*. Epilepsia 1996; 37: 879–91.
13 Traub RD, Wong RKS. Cellular mechanisms of neuronal synchronization in epilepsy. Science 1982; 216: 745–7.
14 Scanziani M, Gahwiler BH, Thompson SM. Presynaptic inhibition of excitatory synaptic transmission by muscarinic and metabotropic glutamate receptor activation in the hippocampus: are Ca^{2+} channels involved? Neuropharmacology 1995; 34: 1549–57.
15 Lindstrom J. Neuronal nicotinic acetylcholine receptors. Ion Channels 1996; 4: 377–450.
16 Paterson D, Nordberg A. Neuronal nicotinic receptors in the human brain. Prog Neurobiol 2000; 61: 75–111.
17 Pettit DL, Augustine GJ. Using caged compounds to map functional neurotransmitter receptors. In: Totowa NJ. Ion-channel localization. Humana Press Inc; 2001.
18 Pettit DL, Shao Z, Yakel JL. Beta-Amyloid1-42 peptide directly modulates nicotinic receptors in the rat hippocampal slice. J Neurosci 2001; 21: 1–5.
19 Liu Q, Wu J. Neuronal nicotinic acetylcholine receptors serve as sensitive targets that mediate beta-amyloid neurotoxicity. Acta Pharmacol Sin 2006; 27: 1277–86.
20 Goto Y, Niidome T, Hongo H, Akaike A, Kihara T, Sugimoto H. Impaired muscarinic regulation of excitatory synaptic transmission in the appswe/ps1de9 mouse model of Alzheimer's disease. Eur J Pharmacol 2008; 583: 84–91.
21 Auerbach JM, Segal M. Muscarinic receptors mediating depression and long-term potentiation in rat hippocampus. J Physiol 1996; 492: 479–93.
22 Rezek IA, Roberts SJ. Stochastic measures for physiological signals. IEEE Trans Biomed Eng 1998; 45: 1186–91.
23 Wu J, Fisher RS. Hyperthermic spreading depressions in the immature rat hippocampal slice. J Neurophysiol 2000; 84: 1355–60.
24 Wu J, Javedan SP, Ellsworth K, Smith K, Fisher RS. Gamma oscillation underlies hyperthermia-induced epileptiformlike spikes in immature rat hippocampal slices. BMC Neurosci 2001; 2: 18–24.
25 Dickinson R, Awaiz S, Whittington MA, Lieb WR, Franks NP. The effects of general anaesthetics on carbachol-evoked gamma oscillations in the rat hippocampus *in vitro*. Neuropharmacology 2003; 44: 864–72.
26 Faulkner HJ, Traub RD, Whittington MA. Disruption of synchronous gamma oscillations in the rat hippocampal slice: a common mechanism of anaesthetic drug action. Br J Pharmacol 1998; 125: 483–92.
27 Traub RD, Whittington MA, Buhl EH, Jefferys JGR, Faulkner HJ. On the mechanisms of the gamma/beta shift in neuronal oscillations induced in rat hippocampal slices by tetanic stimulation. J Neurosci 1999; 19: 1088–105.
28 Javedan SP, Fisher RS, Eder HG, Smith K, Wu J. Cooling abolishes neuronal network synchronization in rat hippocampal slices. Epilepsia 2002; 43: 574–80.
29 Lempel A, Ziv J. On the complexity of finite sequences. IEEE Trans Information Theory 1976; IT-22: 75–88.
30 Hu J, Gao J, Principe J. Analysis of biomedical signals by the lempel-ziv complexity: the effect on finite data size. IEEE Trans Biomed Eng 2006; 53: 2606–9.
31 Amigo JM, Szczepanski J, Wajnryb E, Sanchez-Vives MV. Estimating the entropy rate of spike trains via lempel-ziv complexity. Neural Comput 2004; 16: 717–36.
32 Aboy M, Hornero R, Abasolo D, Alvarez D. Interpretation of the Lempel-Ziv complexity measure in the context of biomedical signal analysis. IEEE Trans Biomed Eng 2000; 53: 2282–8.
33 Williams JH, Kauer JA. Properties of carbachol-induced oscillatory activity in rat hippocampus. J Neurophysiol 1997; 78: 2631–40.
34 Ferenets R, Lipping T, Anier A, Jantti V, Melto S, Hovilehto S. Comparison of entropy and complexity measures for the assessment of depth of sedation. IEEE Trans Biomed Eng 2006; 53: 1067–77.
35 Kaplan DT. Exceptionional evidence of determinism. Physica D 1994; 73: 38–48.
36 Radhakrishnan N, Wilson JD, Lowery C, Murphy P, Eswaran E. Testing for nonlinearity of contraction segments in uterine electromyography. Int J Bifurcation Chaos 2000; 10: 2785–90.
37 Nagarajan R. Quantifying physiological data with Lempel-Ziv

complexity-certain issues. IEEE Trans Biomed Eng 2002; 49: 1371–3.
38 Kurths J, Schwarz U, Witt A, Krampe RT, Abel M. Measures of complexity in signal analysis, chaotic, fractal and nonlinear signal processing. AIP 1995; 375: 33–54.
39 Hao BL. Elementary symbolic dynamics and chaos in dissipative systems. Singapore: World Scientific.
40 Kaspar F, Schuster HG. Easily calculable measure for the complexity of spatiotemporal patterns. Phys Rev 1987; 36A: 842–8.
41 Tang XZ, Tracy ER, Boozer AD, deBrauw A, Brown R. Symbol sequence statistics in noisy chaotic signal reconstruction. Chaos 1995; 51: 3871–89.
42 Radhakrishnan N, Wilson JD, Loizou P. An alternate partitioning technique to quantify the regularity of complex time series. Int J Bifurcation Chaos 2000; 10: 1773–9.
43 Zhang X, Zhu Y, Thakor NV, Wang Z. Detecting ventricular tachycardia and fibrillation by complexity measure. IEEE Trans Biomed Eng 1984; BME-31: 770–8.
44 Zhang X, Roy RJ. Detecting movement during anesthesia by EEG complexity analysis. Med Biol Eng Comput 1999; 37: 327–34.
45 Orlov YL, Potapov VN. Complexity: an internet resource for analysis of DNA sequence complexity. Nucleic Acids Res 2004; 32: W628–W633.
46 Gusev VD, Nemytikova LA, Chuzhanova NA. On the complexity measures of genetic sequences. Bioinformatics 1999; 15: 994–9.
47 Stern L, Allison L, Coppel RL, Dix TI. Discovering patterns in plasmodium falciparum genomic DNA. Mol Biochem Parasitol 2001; 118: 175–86.
48 Szczepaski J, Amigó JM, Wajnryb E, Sanchez-Vives MV. Application of Lempel-Ziv complexity to the analysis of neural discharges. Network 2003; 14: 335–50.
49 Amigó JM, Szczepaski J, Wajnryb E, Sanchez-Vives MV. Estimating the entropy rate of spike trains via Lempel-Ziv complexity. Neural Comput 2004; 16: 717–36.
50 Otu HH, Sayood K. A new sequence distance measure for phylogenetic tree construction. Bioinformatics 2003; 19: 2122–30.
51 Wu X, Xu J. Complexity and brain function. Acta Biophys Sin 1991; 7: 103–6.
52 Xu J, Liu Z, Liu R, Yang QF. Information transformation in human cerebral cortex. Physica D 1997; 106: 363–74.
53 Abásolo D, Hornero R, Gómez C, García M, López M. Analysis of EEG background activity in Alzheimer's disease patients with Lempel-Ziv complexity and central tendency measure. Med Eng Phys 2006; 28: 315–22.
54 Radhakrishnan N, Gangadhar B. Estimating regularity in epileptic seizure time-series data. IEEE Eng Med Biol Mag 1998; 17: 89–94.
55 Zhang XS, Zhu YS, Zhang XJ. New approach to studies on ECG dynamics: extraction and analyses of QRS complex irregularity time series. Med Biol Eng Comput 1997; 35: 467–73.
56 Aboy M, Hornero R, Abasolo D, Alvarez D. Interpretation of the Lempel-Ziv complexity measure in the context of biomedical signals. IEEE Trans Biomed Eng 2006; 53: 2282–8.
57 Szczepaski J, Amigó JM, Wajnryb E, Sanchez-Vives MV. Characterizing spike trains with lempel-ziv complexity. Neurocomputing 2004; 58–60: 79–54.
58 Bellucci A, Luccarini I, Scali C, Prosperi C, Giovannini MG, Pepeu G, *et al*. Cholinergic dysfunction, neuronal damage and axonal loss in TgCRND8 mice. Neurobiol Dis 2006; 23: 260–72.
59 Billings LM, Oddo S, Green KN, Mc Gaugh JL, LaFerla FM. Intraneuronal Aβ causes the onset of early Alzheimer's disease-related cognitive deficits in transgenic mice. Neuron 2005; 45: 675–88.
60 Machova E, Jakubik J, Michal P, Oksman M, Iivonen H, Tanila H, *et al*. Impairment of muscarinic transmission in transgenic appswe/ps1de9 mice. Neurobiol Aging 2008; 29: 368–78.
61 Goto Y, Niidome T, Hongo H, Akaike A, Kihara T, Sugimoto H. Impaired muscarinic regulation of excitatory synaptic transmission in the APPswe/PS1DE9 mouse model of Alzheimer's disease. Eur J Pharmacol 2008; 583; 84–91.
62 Bellucci A, Rosi MC, Grossi C, Fiorentini A, Luccarini I, Casamenti F. Abnormal processing of tau in the brain of aged TgCRND8 mice. Neurobiol Dis 2007; 27: 328–38.
63 Seger R, Krebs EG. The MAPK signaling cascade. FASEB J 1995; 9: 726–35.
64 Sweatt JD. The neuronal map kinase cascade: a biochemical signal integration system subserving synaptic plasticity and memory. J Neurochem 2001; 76: 1–10.
65 Dineley KT, Westerman M, Bui D, Bell K, Ashe KH, Sweatt JD. Beta-amyloid activates the mitogen-activated protein kinase cascade via hippocampal alpha7 nicotinic acetylcholine receptors: *in vitro* and *in vivo* mechanisms related to Alzheimer's disease. J Neurosci 2001; 21: 4125–33.
66 Rosenblum K, Futter M, Jones M, Hulme EC, Bliss TV. ERKI/II regulation by the muscarinic acetylcholine receptors in neurons. J Neurosci 2000; 20: 977–85.
67 Sweatt JD. Mitogen-activated protein kinases in synaptic plasticity and memory. Curr Opin Neurobiol 2004; 14: 311–7.
68 Giovannini MG. The role of the extracellular signal-regulated kinase pathway in memory encoding. Rev Neurosci 2006; 17: 619–34.